Solar-Terrestrial Physics. 2025, vol. 11, iss. 2, pp. 12–18. DOI: 10.12737/stp-112202502. © 2025 V.M. Fedorov, D.M. Frolov. Published by INFRA-M Academic Publishing House

DOI: 10.12737/stp-112202502

Received October 17, 2024
Accepted January 20, 2025

CHANGE IN EARTH'S SOLAR CLIMATE OVER THE PERIOD FROM 1900 TO 2100

V.M. Fedorov
Lomonosov Moscow State University, Moscow, Russia, fedorov.msu@mail.ru

D.M. Frolov
Lomonosov Moscow State University, Moscow, Russia, denisfrolovm@mail.ru

Abstract. The paper presents the results of the analysis of changes in Earth's solar climate over the period from 1900 to 2100. It has been determined that the annual meridional gradient of irradiation intensity from 1900 to 2100 and latitudinal differences in the Earth irradiation intensity increase. A relative increase in winter irradiation intensity for the hemispheres is observed in the regions where extratropical cyclones develop, which may contribute to the activation of cyclonic processes in the atmosphere in the winter half-year. In the Northern Hemisphere, seasonal differences in the irradiation intensity increase during the period of interest, whereas in the Southern Hemisphere they smooth out.

Meridional contrasts in irradiation in the summer half-year increase in the Southern and Northern hemispheres; in the winter half-year in the Northern Hemisphere, meridional contrasts in irradiation decrease; in the Southern Hemisphere, they increase. Insolation seasonality increases slightly in the Northern Hemisphere and increases in the Southern Hemisphere. The transfer of radiative heat from the summer Southern Hemisphere to the winter Northern Hemisphere prevails. There is, however, a tendency for it to decrease.

Keywords: Earth's solar climate, variations of incoming solar radiation, insolation contrast, insolation seasonality, interhemispheric heat exchange.

INTRODUCTION

The solar (mathematical) climate is understood as the theoretically calculated input and distribution of solar energy on the upper limit of the atmosphere (ULA) or on Earth's surface in the absence of the atmosphere [Milankovich, 1939; Monin, Shishkov, 2000]. Thus, ULA is the starting point of the shortwave radiation coming to Earth and Earth's radiation balance, surface, and atmosphere.

Redistribution of radiative heat in the atmosphere and ocean is associated with heat exchange mechanisms. The main ones are the inter-latitudinal heat exchange — meridional radiative heat transfer from the equatorial region to polar regions (the heat engine of the first kind); heat exchange in the ocean—continent system linked to seasonal changes in heat source and sink areas (the heat engine of the second kind) [Shuleikin, 1953]; heat exchange in the ocean—atmosphere system; interhemispheric heat exchange [Sidorenkov, 2002], etc. An important factor in regulating Earth's thermal regime is the atmosphere composition (primarily the water vapor content) that determines the albedo (reflection of shortwave radiation coming from the Sun), the greenhouse effect of the planet and its change [Smirnov, 2021]. The radiative heat transfer intensity is mainly related to changes in Earth's solar climate driven by astronomical factors [Monin, Shishkov, 1979, 2000; Fedorov, 2018, 2023; Fedorov, 2020, 2022].

Calculations taking into account periodic disturbances of elements of the Earth orbit, the axial tilt, and their associated high-frequency variations in solar radiation were performed at A.I. Voeikov Main Geophysical Observatory (MGO) [Borisenkov et al., 1983]. High-frequency radiation variations are studied in Belgium at G. Lemaitre Institute of Astronomy and Geophysics. [Loutre et al., 1992; Bertrand et al., 2002; Berger et al., 2010]. However, calculations with 1-day time resolution were made, firstly, for individual parallels; secondly, only for four (equinoxes and solstices) or five (cardinal points and a point with a heliocentric longitude of 120°) days per year. Nowadays, high-time-resolution insolation calculations have been carried out in [Cionco, Soon, 2017] for 12 thousand years in the past (according to astronomical ephemeris DE-431). The authors calculated solar radiation with daily resolution also for individual parallels and without taking into account changes in the duration of the tropical year.

In calculations of high-frequency (periodic) insolation variations, our approach differs from the methods developed by E.P. Borisenkov, M.-F. Loutre, S. Bertrand, and their colleagues in 1) the initial astronomical data used for the calculations; 2) various calculations of insolation relative to Earth's surface; 3) the time interval covered by the calculations. As initial data, these authors utilized ephemerides calculated at the Institute of Theoretical Astronomy of the USSR Academy of Sciences [Borisenkov et al., 1983]. The initial data for calculations performed by Belgian researchers [Loutre et al., 1992; Bertrand et al., 2002] was the ephemerides VSOP82 [Bretagnon, 1982]. Our calculations use the JPL (Jet Propulsion Laboratory) Planetary and Lunar Ephemerides DE-441 [Folkner et al., 2014; https://ssd.jpl.nasa.gov/].

When calculating the insolation, our predecessors identified Earth's surface with a sphere, and the calculations were made only for individual parallels. Borisenkov et al. [1983] obtained the values only for 20°,

40°, 60°, and 80° N. Loutre et al. [1992] carried out calculations (for mid-July, more precisely, for a point with a geocentric ecliptic longitude of 120°) only for 65° N. For equinoxes and solstices, insolation was estimated only for 0°, 30°, 60°, and 90° in each hemisphere. Recall that the geocentric ecliptic longitude of the Sun is an angle between directions from the center of Earth to the vernal equinox and the Sun. Points of the vernal and autumnal equinoxes are points of intersection of the plane of the Earth orbit (ecliptic) with the plane of the celestial equator. Bertrand et al. [2002] calculated irradiation for the 65°–70° N zone by averaging values obtained for the parallels bounding it (65° and 70° N). In our calculations, Earth's surface was approximated by an ellipsoid. The incoming radiation was calculated not for individual parallels, but for the surface of individual latitude zones (1° latitude resolution), hemispheres, and entire Earth. In addition, we obtained quantitative characteristics of the influence of the shape of Earth on the nature of irradiation of its surface [Fedorov et al., 2020].

The time resolution in calculations of high-frequency insolation variations in [Borisenkov et al., 1983] is ~1 day. Their calculations are, however, presented only for the winter and summer half-years and only for the Northern Hemisphere in 1800–2100. Loutre et al. [1992] carried out the calculations on an interval of 5 000 years in the past with an annual resolution and only for July (a separate point with a geocentric ecliptic longitude of 120°), equinoxes, and solstices. In [Bertrand et al., 2002], insolation calculations cover the previous millennium, but only for July and with annual resolution. Furthermore, the solar constant in our calculations was assumed to be 1361 W/m^2 [Kopp, Lean, 2011]; in the works of our predecessors, 1368 W/m^2 [Bertrand et al., 2002], 1367 W/m^2 [Borisenkov et al., 1983; Loutre et al., 1992].

Our calculations are based on high-precision ephemerides, a new solar constant (1361 W/m^2) [Kopp, Lean, 2011], and cover in more detail the time interval of 20 thousand years and the entire Earth surface. In our calculations, Earth is not identified with a sphere, but is approximated by an ellipsoid. The error in calculating irradiation of the sphere and the ellipsoid of equal volume (differing in surface curvature) is comparable to 11-year solar cycle variations (at present) [Fedorov et al., 2020]. Thus, the calculations fill the spatial and temporal gaps in insolation calculations for the period from 10 000 BC to 10 000 AD. Realism and reliability of the results of modeling of the nonlinear oscillatory natural system depend on completeness and accuracy of initial radiation data. When modeling nonlinear processes in the natural system, the accuracy of reproduction and the depth of the forecast are reduced due to an increase in errors and uncertainties associated with insufficient completeness and accuracy of initial radiation data. In this regard, the data on Earth irradiation (Incoming Solar Radiation) we calculated with high spatial and temporal resolution can become components of the radiation block of physico-mathematical climate models, which will contribute to improvement of this high-tech instrumentation, as well as to increase in the reliability and depth of climate forecasts.

In this case, the results easily take into account solar radiation variations associated with solar activity variation. To do this, it is enough to divide available reconstructed *TSI* (total solar irradiance) values by the value of 1361 W/m^2 we employ, and then multiply the calculated insolation values by the obtained coefficients. Thus, variations of different physical nature in changes in the total flux of incoming solar radiation are taken into account [Fedorov et al., 2021; Fedorov, 2023].

1. CALCULATION METHOD

The calculations have been performed using data from high-precision astronomical ephemerides (DE-441) [Folkner et al., 2014; https://ssd.jpl.nasa.gov/] for the upper limit of the atmosphere (or Earth's surface excluding the atmosphere) in the range from 10 000 BC to 10 000 AD. The initial astronomical data for solar insolation calculations includes declination and ecliptic longitude of the Sun, the distance from Earth to the Sun, and the difference between Coordinate Time and Universal Time. Earth's surface was approximated by an ellipsoid (Geodetic Reference System – 1980, GRS80) with half-axis lengths of 6378137 (large) and 6356752 m (small). In general, the calculation algorithm is represented by the expression

$$I_{nm}(\varphi_1, \varphi_2) = \\ = \int_{\varphi_1}^{\varphi_2} \left(\sigma(\varphi) \left(\int_{-\pi}^{\pi} \Lambda(t, \varphi, \alpha) d\alpha \right) d\varphi \right) dt, \quad (1)$$

where I is the incoming solar radiation for the elementary nth fragment of the mth tropical year (J); σ is the area multiplier (m^2) that is used to calculate the area differential $\sigma(\varphi) d\alpha\, d\varphi$ — the area of an infinitesimal trapezoid cell of the ellipsoid; α is the hour angle; φ_1, φ_2 are geographical latitudes in radians; $\Lambda(t, \varphi, \alpha)$ is solar radiation at a given moment at a given location on the surface of the ellipsoid (W/m^2); t is time (s). The integration steps were 1° in longitude, 1° in latitude, and 1/360 of the duration of the tropical year with regard to its change. Solar activity variation was ignored in the calculations. The solar constant (mean long-term *TSI*) was assumed to be 1361 W/m^2 [Kopp, Lean, 2011]. The method for calculating the solar energy coming to Earth's ellipsoid is detailed in [Fedorov, 2018; Fedorov, Kostin, 2020].

2. IRRADIATION INTENSITY VARIATION ACROSS LATITUDE ZONES

We have analyzed the dynamics of Earth's solar climate for the XX–XXI centuries. Variation in the intensity of annual and semiannual irradiation of Earth and hemispheres over the period 1900–2100 is insignificant. In this regard, the paper examines the change in intensity characteristics of Earth's annual (Figure 1) and seasonal irradiation within 5° latitude zones.

In 5° latitude zones, the annual irradiation intensity varies on average from maximum in the region 5° N – 5° S (415.1 W/m^2) to minimum (173.0 W/m^2) in polar latitude zones (85°–90° N and 85°–90°S). We estimated variations in annual irradiation intensity in 5° latitude zones for the period 1900–2100 (Figure 2).

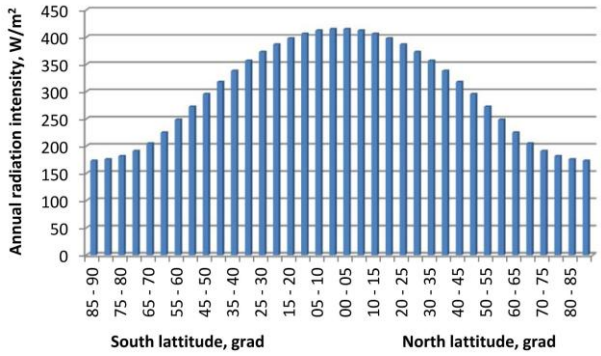

Figure 1. Average long-term intensity of Earth's annual irradiation over the period 1900–2100

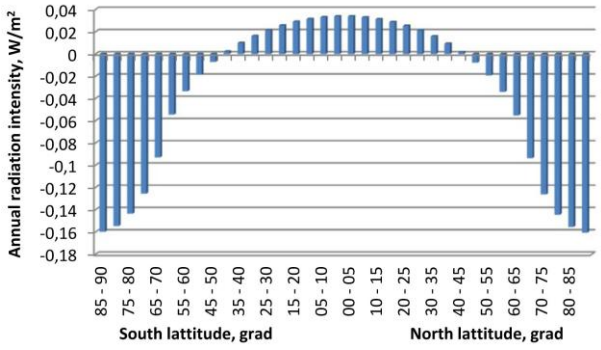

Figure 2. Variation in Earth's annual irradiation intensity over the period 1900–2100

Annual irradiation intensity increases in the region from 45° N to 45° S. The maximum increase in the annual irradiation intensity is observed in the range 5° N – 5° S (0.034 W/m^2 or 0.008 % of the average irradiation over 1900–1909). A decrease in the annual irradiation intensity is typical for latitudes 45°–90° in each hemisphere. The maximum decrease in the annual irradiation intensity (–0.160 W/m^2 or 0.09 %) is peculiar to polar cells (85°–90° in each hemisphere). Variation in Earth's annual irradiation intensity in relative units (as a percentage of the corresponding averages for the first decade 1900–1909) is similar to the distribution shown in Figure 2. The obtained pattern of variation in the annual irradiation of Earth by latitude is explained by a decrease in the angle of the rotation axis [Milankovich, 1939]. Thus, the meridional gradient of the annual irradiation intensity increases.

The intensity of Earth's semiannual irradiation is characterized by the distribution illustrated in Figure 3.

During the first astronomical half-year, maximum irradiation intensity average for the period 1900–2100 is observed in 20°–25° and 25°–30° N (443.503 and 443.326 W/m^2 respectively). There are two minima: in the northern polar cell (85°–90° N, 338.027 W/m^2) and in the southern one (85°–90° S, 1.016 W/m^2). During the second astronomical half-year, irradiation intensity maxima occur in 20°–25° S and 25°–30° S (462.280 and 462.096 W/m^2 respectively). Minima are also recorded in the polar regions (85°–90° S, 353.337 W/m^2 and 85°–90° N, 1.059 W/m^2). Variation in the semiannual irradiation intensity over the period from 1900 to 2100 is more complex than variation in the annual one (Figure 4).

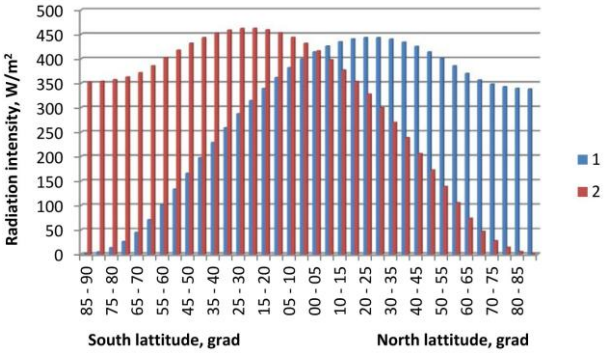

Figure 3. Average long-term intensity of Earth's semiannual irradiation over the period 1900–2100: 1, 2 — the first and second astronomical half-years

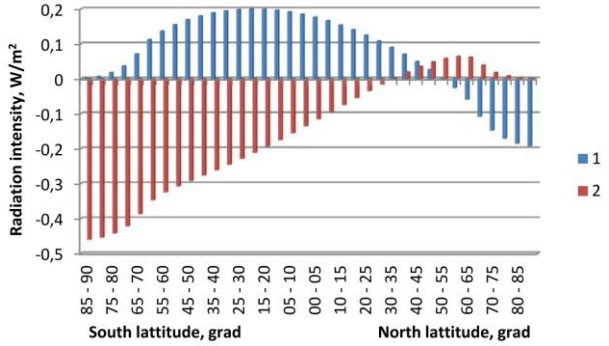

Figure 4. Change in Earth's semiannual irradiation intensity over the period 1900–2100: 1, 2 — the first and second astronomical half-years

During the first astronomical half-year, the irradiation intensity increases in the latitudinal region from the South Geographic Pole to 50°–55° N. In the latitude zone 55°–90° N, the irradiation intensity decreases. Its maximum increase during the first astronomical half-year is typical for 20°–25° S (0.200 W/m^2). The maximum decrease in the irradiation intensity during the first astronomical half-year is observed in the northern polar zone (85°–90° N, 0.193 W/m^2). During the second astronomical half-year, the irradiation intensity decreases in the region from 25°–30° S to the South Geographic Pole, where it reduces to the maximum (by 0.461 W/m^2). The region 30°–90° N is characterized by an increase in the irradiation intensity during the second astronomical half-year, with a maximum (by 0.064 W/m^2) in the latitude zone 55°–60° N. The pattern of the relative changes is similar in magnitude, but differs in numerical values from irradiation intensity variations shown in absolute units (Figure 5).

The regions where the irradiation intensity increases and decreases during the half-years are similar to those shown in Figure 4. There is, however, a shift in the domain of extreme values in the irradiation intensity variation. During the first astronomical half-the year, for example, maximum relative increases in the irradiation intensity occur in the latitudinal zones 60°–65° S and 65°–70°S (0.159 and 0.158 % respectively). Its maximum increase during the second astronomical half-year is observed in 60°–65° N and 65°–70° N (by 0.084 %). Thus, a relative increase in the semiannual irradiation

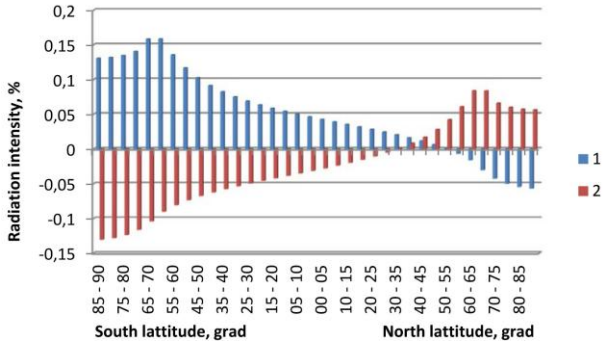

Figure 5. Change in Earth's semiannual irradiation intensity over the period 1900–2100 as a percentage of the corresponding averages for the first decade 1900–1909: 1, 2 — the first and second astronomical half-years

intensity takes place in the region of extratropical cyclone development [Poghosyan, 1976], which may contribute to an increase in the frequency and intensity of cyclonic processes in the atmosphere.

3. IRRADIATION INTENSITY VARIATION BY SEASONS

The average annual course of the irradiation intensity in the Northern and Southern hemispheres is asymmetric (Figure 6).

In the Northern Hemisphere, the maximum average long-term irradiation intensity is recorded in the third and forth astronomical months (456.222 and 454.453 W/m^2). In the Southern Hemisphere, the minimum irradiation intensity is observed during these months (204.511 and 203.718 W/m^2 respectively). The minimum average long-term irradiation intensity in the Northern Hemisphere occurs in the ninth and tenth astronomical months (216.803 and 217.623 W/m^2 respectively). In the Southern Hemisphere, the irradiation intensity is maximum during these months (483.642 and 485.471 W/m^2 respectively). Thus, irradiation intensity maxima and minima occur during equinoxes.

The annual course of the irradiation intensity in the hemispheres changes differently (Figure 7).

In the Northern Hemisphere in the first three and last three months of the tropical year from 1900 to 2100, the irradiation intensity increases. The maximum increase occurs in the first and 12th months of the tropical year (0.671 and 0.519 W/m^2 respectively). In terms of mean irradiation intensity for the first decade (1900–1909), this increase is 0.179 % and 0.168 % respectively. The irradiation intensity in the Northern Hemisphere decreases from the forth to the ninth astronomical month. Its maximum decreases in the Northern Hemisphere are typical for the sixth (by 0.623 W/m^2 or 0.169 %) astronomical month. In the Southern Hemisphere, the regions of irradiation intensity increase and decrease relative to the Northern Hemisphere are shifted by a month. The decrease is observed here from the fifth to tenth astronomical month, and the increase occurs from the first to forth month, as well as in the eleventh and twelfth months. The maximum reduction in the irradiation intensity takes place in the Southern Hemisphere in the seventh (0.741 W/m^2 or 0.197 %) and eighth (0.829 W/m^2 or 0.187 %) astronomical months. Its maximum increase occurs in the first (0.606 W/m^2 or 0.199 %) and twelfth (0.564 W/m^2 or 0.148 %) months of the tropical year. The change in the annual course in relative values in the hemispheres has similarities in the signs of irradiation intensity variation and differences in its corresponding increases or decreases.

To obtain a general pattern of the spatial and temporal variations in the irradiation intensity, we have formed irradiation intensity matrices for 1900, 2000, and 2100. By subtracting the matrix of 1900 from the matrix of 2000 (Figure 8, *a*) and the matrix of 2000 from the matrix of 2100 (Figure 8, *b*), we obtained patterns of spatial and temporal variations in Earth's irradiation intensity for the current and previous centuries.

4. CHANGES OF CONTRAST IN IRRADIATION INTENSITY ON THE UPPER LIMIT OF THE ATMOSPHERE

The insolation coming to the upper limit of the atmosphere (radiative heat) is transferred by radiation. In the natural system, the radiative heat is generally transferred by water and air masses. Intensity of this transfer is, however, regulated by the meridional, seasonal, and interhemispheric contrasts in Earth irradiation on the upper limit of the atmosphere [Fedorov, 2023].

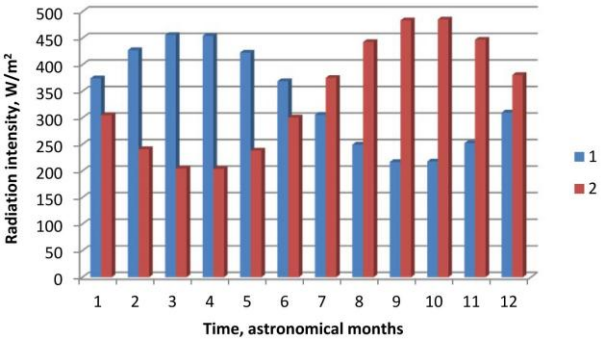

Figure 6. Average long-term irradiation intensity in the hemispheres over the period from 1900 to 2100: 1, 2 — Northern and Southern hemispheres

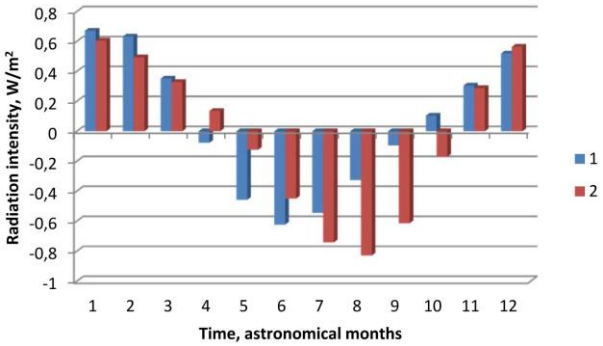

Figure 7. Changes in the annual course of Earth's irradiation intensity over the period from 1900 to 2100: 1, 2 — Northern and Southern hemispheres

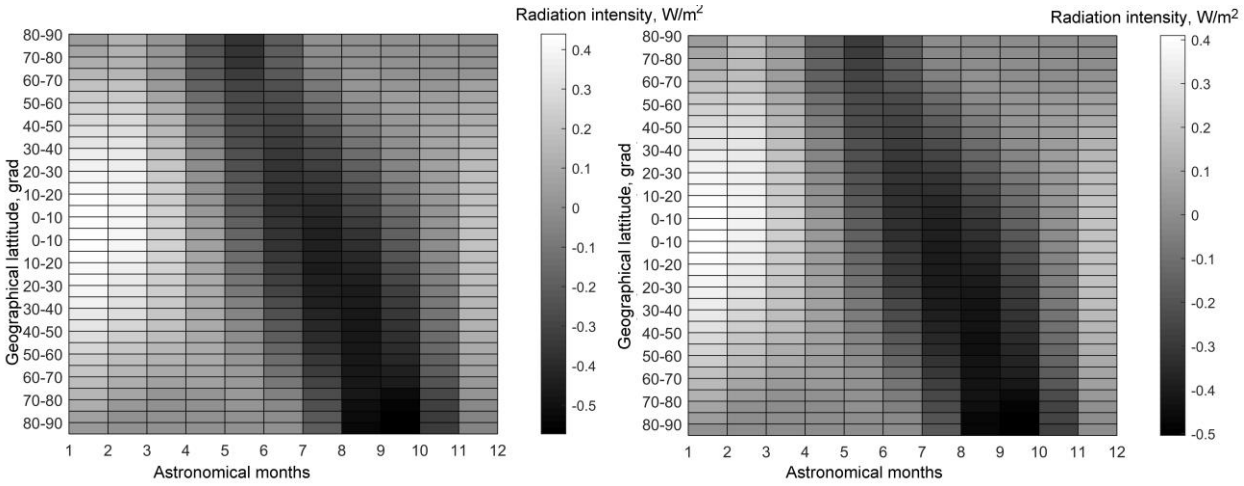

Figure 8. Spatial and temporal variations in Earth's irradiation intensity over the periods 1900–2000 (*a*) and 2000–2100 (*b*)

We estimated the change in the insolation contrast (IC), which regulates the meridional radiative heat transfer to the upper limit of the atmosphere, over the period 1900–2100. Annual IC for the hemispheres was calculated as irradiation intensity difference in 00°–45° (heat source) and 45°–90° (heat sink). This characteristic generically indicates the change in the meridional insolation gradient (MIG) in the radiative heat source and sink areas [Fedorov, 2022; Fedorov, 2023]. The summer and winter IC values for the hemispheres were calculated taking into account the seasonal shift of the heat source and sink areas. For the summer hemisphere, the heat source area was assumed to be 0°–55° latitude; for the sink area, 55°–90°. For the winter hemisphere, the source area was limited to the range from the 0°–35° latitude; the sink area extended to the 35°–90° latitude.

Annual IC (the same in the hemispheres) increases slightly over the period from 1900 to 2100. With an average long-term value of 140.490 W/m^2, the increase in annual IC is limited to 0.1 W/m^2. More significant changes are typical for seasonal (summer and winter) IC. Seasonal ICs are closely related. The relationship between summer ICs is positive (0.996 correlation coefficient); between winter ICs, negative (–0.983). Summer and winter ICs in the Northern Hemisphere exhibit a high negative correlation (–0.976); in the Southern Hemisphere, a positive one (0.909). Winter IC in the Northern Hemisphere from 1900 to 2100 is 3.232 times higher than summer IC; in the Southern Hemisphere, 2.975 times. The average long-term winter IC in the Northern Hemisphere is 216.220; in the Southern Hemisphere, 207.438 W/m^2. Summer average long-term IC is 66.900 in the Northern Hemisphere and 69.733 W/m^2 in the Southern Hemisphere. From 1900 to 2100, winter IC in the Northern Hemisphere decreases by 0.1 W/m^2; in the Southern Hemisphere, it increases by 0.08 W/m^2. From 1900 to 2100, summer IC increases in the Northern (by 0.245 W/m^2) and Southern (0.204 W/m^2) hemispheres (Figure 9). Changes in summer ICs are more than twice as large as changes in winter ICs in the hemispheres.

Thus, the insolation contrast in irradiation of the Northern and Southern hemispheres increases during the summer half-year.

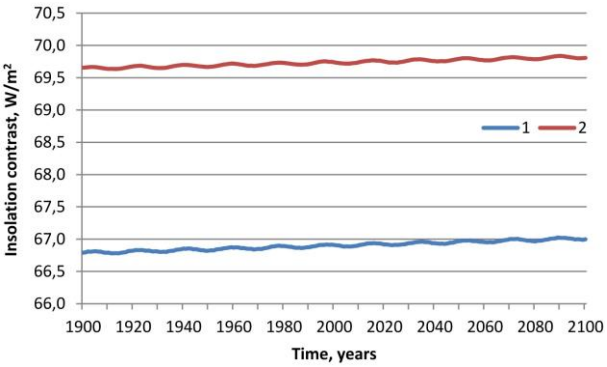

Figure 9. Changes in the summer insolation contrast in the Northern (1) and Southern (2) hemispheres in 1900–2100

During the winter half-year, IC decreases in the Northern Hemisphere and increases in the Southern Hemisphere. Annual and seasonal MIGs, whose generalized characteristic is IC, regulates the meridional radiative heat transfer in Earth's natural system from low latitudes (heat source) to high latitudes (heat sink), i.e. regulates the rate of work of the heat engine of the first kind [Shuleikin, 1953]. In the natural system (in the ocean and atmosphere), the annual meridional energy transfer exceeds 5–7 times annual MIG due to involvement of water and air masses in radiative heat transfer [Palmen, Newton, 1973; Peixoto, Oort, 1984; Fedorov, 2023].

The insolation seasonality (IS) represents the seasonal irradiation contrast of Earth, which regulates the radiative heat transfer in the ocean—continent system due to the seasonal reverse change of heat source and sink areas (the rate of work of the heat engine of the second kind). The insolation seasonality is calculated as the difference between summer and winter irradiation intensity in the hemispheres [Shuleikin, 1953; Monin, 1982]. In 1900–2100, IC increases slightly in the Northern Hemisphere (by 0.156 W/m^2) and decreases in the Southern Hemisphere (by 0.474 W/m^2) (Figure 10). The average long-term IC in the Northern Hemisphere is 158.713; in the Southern Hemisphere, 186.919 W/m^2. It is nevertheless possible that these small changes are enough

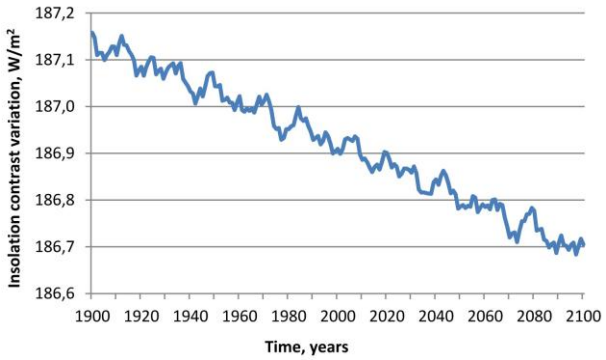

Figure 10. Changes in insolation seasonality in the Southern Hemisphere in 1900–2100

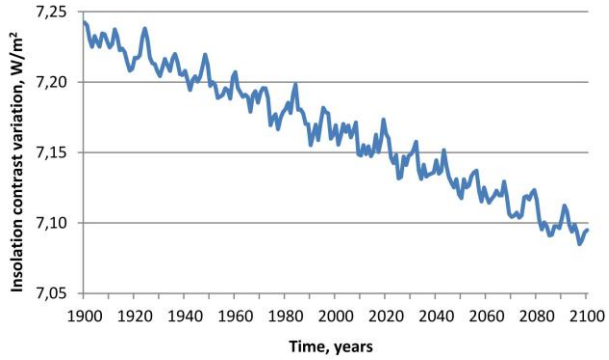

Figure 11. Changes in Earth's insolation seasonality over the period 1900–2100

to regulate the heat exchange in the ocean—continent system (in particular, the intensity of monsoon development).

Thus, seasonal differences in 1900–2100 increase slightly in the Northern Hemisphere, and smooth out in the Southern Hemisphere.

Interhemispheric heat exchange is also considered in terms of irradiation contrast (latitudinal and seasonal). For this purpose, we introduce a solar characteristic of interhemispheric contrast in irradiation, which we call Earth's insolation seasonality (EIS). This characteristic of irradiation governs interhemispheric heat exchange or radiative heat transfer from the summer hemisphere to the winter hemisphere, thereby smoothing out seasonal differences in the solar climate of the hemispheres. EIS is determined from the ratio EIS = (summer irradiation intensity in the Southern Hemisphere – winter irradiation intensity in the Northern Hemisphere) – (summer irradiation intensity in the Northern Hemisphere – winter irradiation intensity in the Southern Hemisphere). In this case, positive EIS values mean that the interhemispheric contrast gradient is directed from the Southern Hemisphere to the Northern Hemisphere, i.e. the radiative heat transfer from the summer Southern Hemisphere to the winter Northern Hemisphere prevails. This is due to the partial shift of the Hadley circulation cell from the winter hemisphere to the summer hemisphere. Over the period from 1900 to 2100, EIS is positive, which reflects the radiative heat transfer from the summer Southern Hemisphere to the winter Northern Hemisphere. Average long-term EIS is 7.165 W/m^2. Yet, while remaining positive, EIS decreases. From 1900 to 2100, EIS decreases by 0.157 W/m^2 (Figure 11).

CONCLUSION

1. We have determined that the annual irradiation of Earth increases in the radiative heat source area 45° N – 45° S and decreases in its sink areas (45°–90° in each hemisphere). The annual meridional insolation gradient increases in 1900–2100 and the latitudinal differences in Earth's irradiation intensity increase.

2. During the first astronomical half-year, maximum relative increases in the irradiation intensity occur in the latitude zones 60°–65° S and 65°–70° S (0.159 and 0.158 % respectively). Its maximum increase during the second astronomical half-year is observed in 60°–65° N and 65°–70° N (by 0.084 %). Thus, a relative increase in the winter irradiation intensity for the hemispheres is observed in areas of extratropical cyclone development, which may contribute to an increase in the intensity of cyclonic processes in the atmosphere (cyclogenesis) during the winter half-year.

3. In the Northern Hemisphere, the irradiation intensity decreases during the winter half-year and increases during the summer half-year. Seasonal differences increase in the Northern Hemisphere during the period under study. In the Southern Hemisphere, the irradiation intensity increases during the winter half-year, and decreases during the summer one. Thus, seasonal differences in the Southern Hemisphere are smoothed out.

4. We have determined trends in changes in contrast characteristics in the latitudinal and seasonal irradiation of Earth and hemispheres. The summer insolation contrast (IC) in the hemispheres increases (by 0.245 in the Northern Hemisphere and by 0.204 W/m^2 in the Southern Hemisphere). Winter IC in the Northern Hemisphere decreases (by 0.117 W/m^2), and the Southern Hemisphere it increases (by 0.079 W/m^2). The insolation seasonality increases slightly in the Northern Hemisphere (by 0.156 W/m^2), and decreases in the Southern Hemisphere (by 0.464 W/m^2). The interhemispheric radiation gradient (positive EIS values) is directed from the summer Southern Hemisphere to the winter Northern Hemisphere. Yet, EIS over the period from 1900 to 2100 decreases by 0.157 W/m^2.

The work was carried out with the support of the state budget themes "Evolution, Current State, and Forecast of Development of the Coastal Zone of the Russian Arctic" (121051100167-1) and "Danger and Risk of Natural Processes and Phenomena" (121051300175-4).

REFERENCES

Berger A., Loutre M.F., Yin Q. Total irradiation during any time interval of the year using elliptic integrals. *Quaternary Sci. Rev*. 2010, vol. 29, pp. 1968–1982. DOI: 10.1016/j.quascirev.2010.05.07.

Bertrand C., Loutre M.F., Berger A. High frequency variations of the Earth's orbital parameters and climate change. *Geophys. Res. Lett*. 2002, vol. 29, no. 18, pp. 40-1–40-3. DOI: 10.1029/2002GL015622.

Borisenkov E.R., Tsvetkov A.V., Agaponov S.V. On some characteristics of insolation changes in the past and the future. *Climatic Change*. 1983, vol. 5, pp. 237–244.

Bretagnon P. Theorie du movement de l'ensemble des planetes.

Solution VSOP82. *Astron. Asrtrophys.* 1982, vol. 114, no. 2, pp. 278–288.
Cionco R.G., Soon W.W-H. Short-term orbital forcing: a quasi-review and a reappraisal of realistic boundary conditions for climate modeling. *Earth-Science Rev.* 2017, vol. 166, pp. 206–222. DOI: 10.1016/j.earscirev.2017.01.013.
Fedorov V.M. *Solar Radiation and the Earth's Climate*. Moscow, Fizmatlit Publ., 2018, 232 p.
Fedorov V.M. Features of the Earth's solar climate changes in the present epoch. *Geomagnetism and Aeronomy*. 2020, vol. 60, no. 7, pp. 993–998.
Fedorov V.M. Insolation contrast and trends in modern climate change. *Geomagnetism and Aeronomy*. 2022, vol. 62, no. 7, pp. 932–937. DOI: 10.1134/S001679322207009X.
Fedorov V.M. Problems of parameterization of the radiation block of physico-mathematical climate models and the possibilities of their solution. *Successes of Physical Sciences*, 2023, vol. 193, no. 9, pp. 971–988. DOI: 10.3367/UFNr.2023.03.039339.
Fedorov V.M., Kostin A.A. The calculation of the Earth's insolation for the 3000 BC-AD 2999. *Springer Geology*. 2020, vol. 1, pp. 181–192. DOI: 10.1007/978-3-030-38177-6_20.
Fedorov V.M., Kostin A.A., Frolov D.M. The influence of the shape of the Earth on the characteristics of the irradiation of the Earth's surface. *Geophysical Processes and the Biosphere*. 2020, vol. 19, no. 3, pp. 119–130. DOI: 10.21455/GPB2020.3-7.
Fedorov V.M., Frolov D.M., Soon W.W-H, Velasco Herrera V.M., Cionco R.G. Role of the radiation factor in global climate events of the late Holocene. *Izvestiya: Atmospheric and Oceanic Physics*. 2021, vol. 57, no. 10, pp. 1239–1253. DOI: 10.1134/S0001433821100030.
Folkner W.M., Williams J.G., Boggs D.H., Park R.S., Kuchynka P., et al. The planetary time series. *Rev. Geophys*. 2014, vol. 40, pp. 3-1–3-41.
Kopp G., Lean J. A new lower value of total solar irradiance: Evidence and climate significance. *Geophys. Res. Lett.* 2011, vol. 37, L01706. DOI: 10.1029/2010GL045777.
Loutre M.F., Berger A., Bretagnon E., Blanc P.-L. Astronomical frequencies for climate research at the decadal to century time scale. *Climate Dynamics*. 1992, vol. 7, pp. 181–194.
Milankovich M. *Mathematical Climatology and Astronomical Theory of Climate Fluctuations*. Moscow-Leningrad, GONTI Publ., 1939, 208 p.
Monin A.S. *Introduction to the Theory of Climate*. Leningrad, Hydrometeoizdat Publ., 1982, 246 p.
Monin A.S., Shishkov Yu.A. *History of Climate*. Leningrad, Hydrometeoizdat Publ., 1979, 408 p.
Monin A.S., Shishkov Yu.A. Climate as a problem of physics. *Successes of Physical Sciences*. 2000, vol. 170, no. 4, pp. 419–445.
Palmen E. Newton Ch. Atmospheric Circulation Systems. Leningrad, Hydrometeoizdat Publ., 1973, 616 p.
Peixoto J.P., Oort A.H. Physics of climate. *Rev. Modern Phys*. 1984, vol. 56, no. 3, pp. 365–429.
Poghosyan H.P. *Cyclones*. Leningrad, Hydrometeoizdat Publ., 1976, 148 p.
Sidorenkov N.S. *Atmospheric Processes and the Rotation of The Earth*. St. Petersburg, Hydrometeoizdat Publ., 2002, 366 p.
Smirnov B.M. Problems of global atmospheric energy. *High Temperature Thermophysics*. 2021, vol 59, no. 4, pp. 589–599. DOI: 10.31857/S0040364421030121.
Shuleikin V.V. *Physics of the Sea*. Moscow, USSR Academy of Sciences Publ., 1953, 990 p.
URL: http://ssd.jpl.nasa.gov (accessed March 10, 2025).

Original Russian version: Fedorov V.M., Frolov D.M., published in Solnechno-zemnaya fizika. 2025, vol. 11, no. 2, pp. 15–21. DOI: 10.12737/szf-112202502.

How to cite this article
Fedorov V.M., Frolov D.M. Change in Earth's solar climate over the period from 1900 to 2100. *Sol.-Terr. Phys*. 2025, vol. 11, iss. 2, pp. 12–18. DOI: 10.12737/stp-112202502.